ME51 Lab 3&4
Teddy Robbins and Rónán Gissler

1. Introduction

The focus of this report is the flow of air through a heat sink composed of a solid base with upraised heat fins. Heat sinks like these are attached to CPUs or other electronic components to keep them cool. This prevents overheating of the electronics which otherwise could cause failure. By studying this flow and how the flow changes when adjustments are made to the structure of the heat sink, engineers can design new heat sinks to more efficiently cool electronic components.

This report examines the impact of the heat fin angle on the flow and heat transfer through the heat sink under forced convection from a fan using COMSOL Multiphysics simulation. In particular, the pressure drop across the heat sink, the thermal resistance of the heatsink, and the average temperature of the CPU die were recorded from simulation data. Understanding this pressure, thermal resistance, and temperature data is important because these parameters are the most important indicators of heat sink efficiency.[1] By exploring how the fin angle can be changed to achieve lower die temperatures through lower static pressures and thermal resistances, more efficient heat sinks can be designed. The research paper used to validate and compare the model against is titled *Experimental study of the heat sink assembly with oblique straight fins*, and is linked here. The authors of the study compare flow and heat transfer data between a heat sink with straight fins and heat sinks with oblique fins (fins oriented at an angle), hereafter referred to as the "straight" and "oblique" models. Unlike the research paper which only uses one oblique model, we analyzed four different angle oblique models including the angle used for the oblique model from the paper.

2. Methods

Geometry:

The heat sink geometry was simulated in 3D to account for flow variations along the length of the heat fins such as the dimensions of the fan relative to the heat sink. To begin, the straight model and oblique model (with a heat fin angle of 71°) from the technical drawings included in the paper were modeled in Solidworks. The models were made parametric so that they could be easily modified if needed. At times the technical drawings disagreed with the text of the paper, so in those cases critical dimensions like fin thickness, fin height, and base dimensions were kept consistent across both oblique and straight models.

In addition to the models replicated from the paper, three additional oblique models were generated using the heat fin angles α = 81°, 61°, and 51°. This resulted in five total models with the heat fin angles α = 90°, 81°, 71°, 61°, and 51°.

To simulate the air domain around the heat sink, a bounding box was added around the heat sink models coincident to the bottom face of the heat sink, offset 1mm from the top of the heat sink, and 10mm from the walls of the heat sink. The dimensions of the bounding box were selected as such to allow for examination of flow characteristics around the heat sink while keeping computation time low.

Technical drawings of the straight model and one oblique model with the heat fin angle used in the paper are displayed inline below.

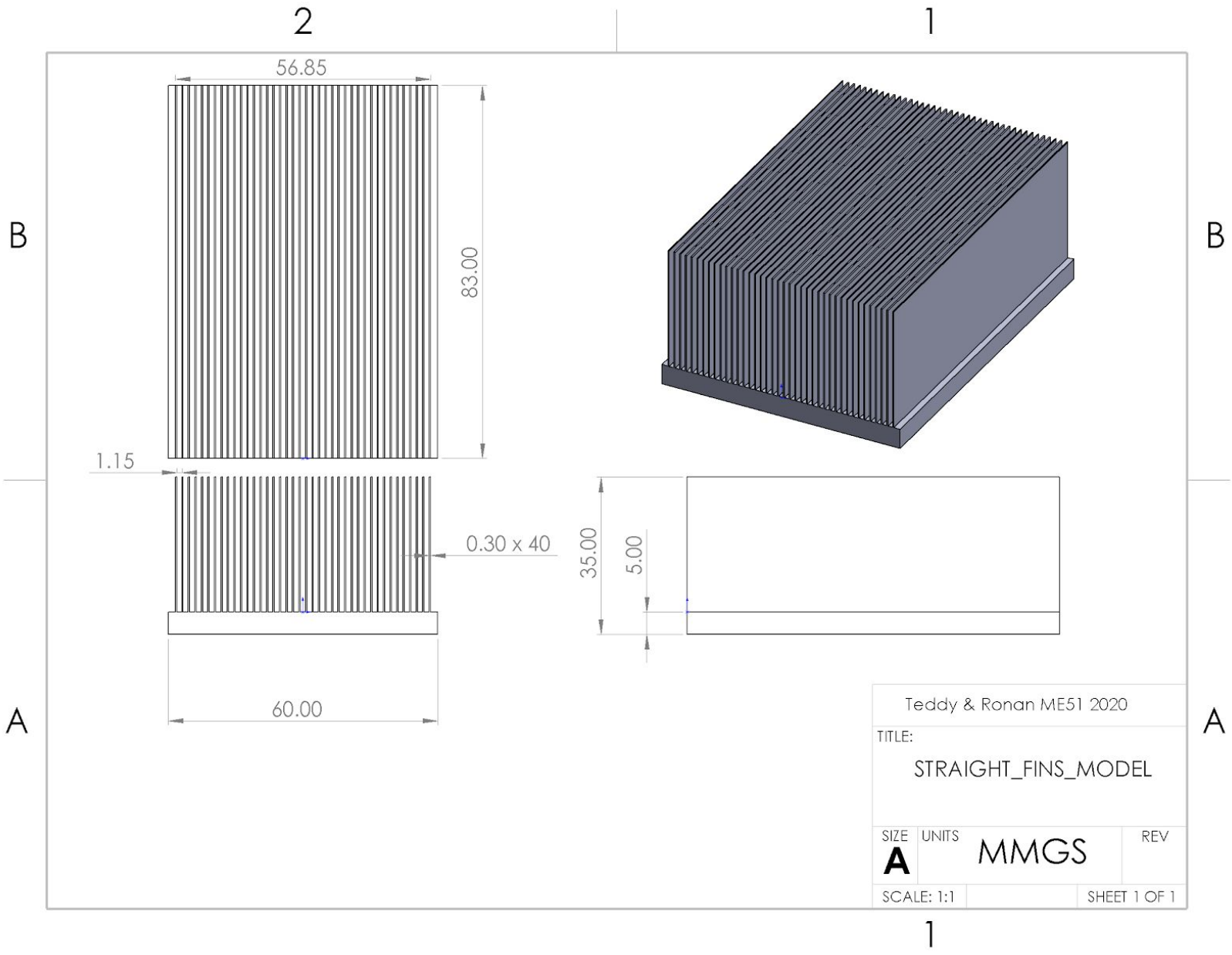

Figure 1. Solidworks Drawing of Straight Fins Heat Sink.
Note that the dimensions for this model were adjusted from the drawings provided in the paper to make the straight and oblique models more comparable.

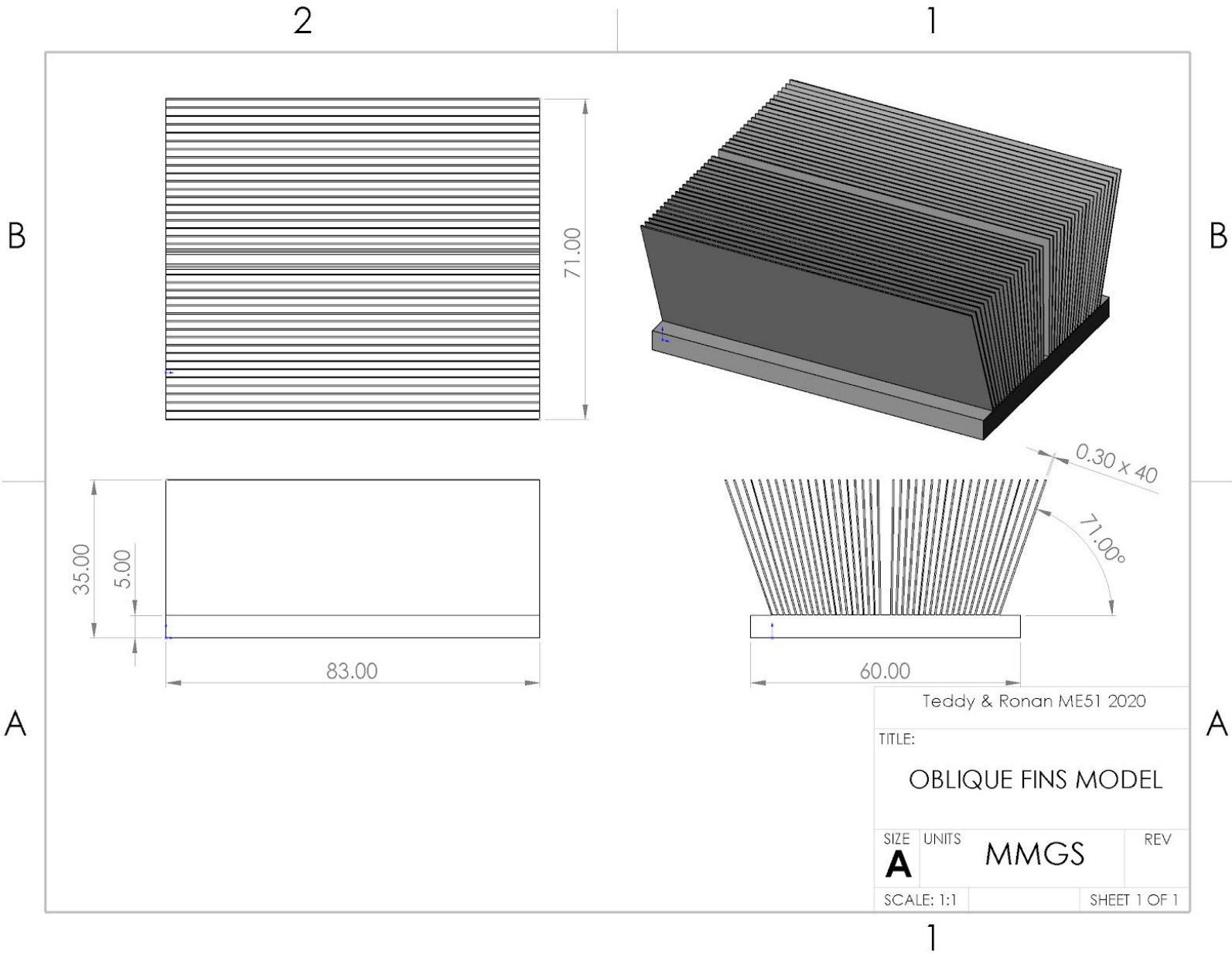

Figure 2. Solidworks Drawing of Oblique Fins (α = 71°) Heat Sink.

Again, note that the dimensions for this model were adjusted from the drawings provided in the paper to make the straight and oblique models more comparable.

Boundary conditions:

To analyze the flow and heat transfer data through the heat sinks, boundary conditions were set for the flow and heat transfer parameters using the Laminar Flow and Heat Transfer in Solids and Fluids modules in COMSOL. A stationary study was used to analyze the system since the heat flux from the CPU and fan speed were both assumed to be constant during operation of the heat sinks.

Laminar Flow:

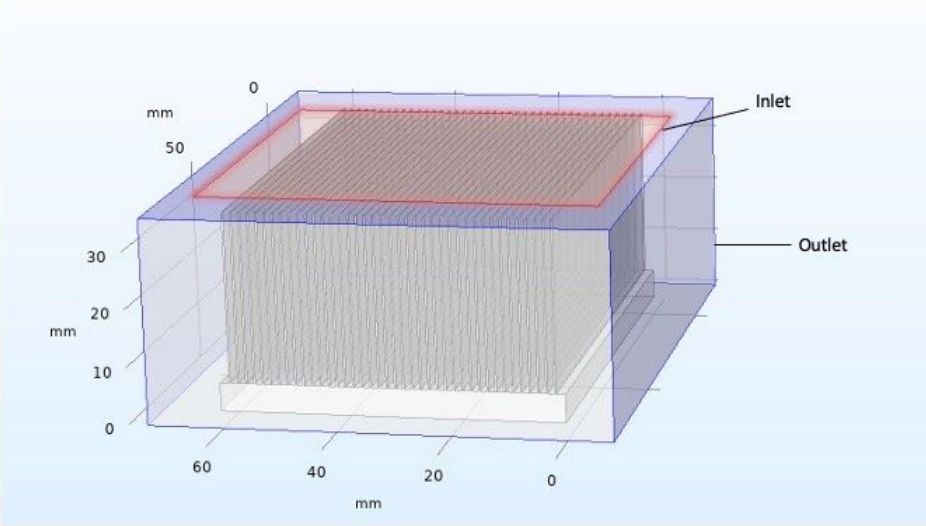

Figure 3. Laminar Flow Boundary Conditions. The pictured heat sink uses straight fins, but the same boundary conditions were used for all fin types.

Simulations were run for three different inlet flow rate conditions: 10, 20, and 30 CFM. Dividing these inlet flow rates by the area through which the fan blows the air (70 x 70 mm^2), inlet flow velocities were calculated to be used as inputs for the inlet condition in the Laminar Flow module.

Inlet Flow Velocity for 10 CFM: $v = \frac{Q}{A} = \frac{10\ ft^3/min}{0.0049\ m^2} \times (\frac{0.3048\ m}{1\ ft})^3 \times \frac{1\ min}{60\ s} = 0.963\ m/s$

Inlet Flow Velocity for 20 CFM: $v = \frac{Q}{A} = \frac{20\ ft^3/min}{0.0049\ m^2} \times (\frac{0.3048\ m}{1\ ft})^3 \times \frac{1\ min}{60\ s} = 1.93\ m/s$

Inlet Flow Velocity for 30 CFM: $v = \frac{Q}{A} = \frac{30\ ft^3/min}{0.0049\ m^2} \times (\frac{0.3048\ m}{1\ ft})^3 \times \frac{1\ min}{60\ s} = 2.89\ m/s$

For each simulation, the calculated inlet velocity was then set as a uniform normal velocity boundary condition over a square surface centered over the heat sink representing the fan of area 70 x 70 mm^2, highlighted in red above in Figure 3.

The Reynolds number was also calculated at the inlets to determine the flow regime so that use of the Laminar Flow module could be validated. The characteristic length selected was the length of the heat sink to be conservative as this was the largest dimension of the heat sink. Since the air flow across the heat sink surface is an external flow, and all calculated Reynolds numbers are less than 10^5, the flow is considered to be laminar.

Reynolds Number for 10 CFM: $Re = \frac{Lv}{\nu} = \frac{(0.083\ m)(0.963\ m/s)}{(1.5\times10^{-5}\ m^2/s)} \approx 5,329$

Reynolds Number for 20 CFM: $Re = \frac{Lv}{\nu} = \frac{(0.083\ m)(1.93\ m/s)}{(1.5\times10^{-5}\ m^2/s)} \approx 10,679$

Reynolds Number for 30 CFM: $Re = \frac{Lv}{\nu} = \frac{(0.083\ m)(2.89\ m/s)}{(1.5\times10^{-5}\ m^2/s)} \approx 15,991$

At the outlets, highlighted in blue above in Figure 3, the boundary condition of atmospheric pressure (zero gauge pressure) with backflow suppressed was used simulating standard room air.

Heat Transfer in Solids and Fluids:

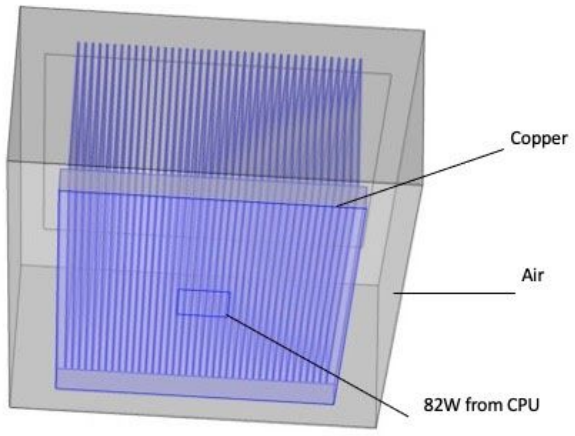

Figure 4. Heat Transfer Boundary Conditions. Again, the pictured heat sink uses straight fins, but the same boundary conditions were used for all fin types.

Using the Heat Transfer in Solids and Fluids module, the heat transfer modes modelled included conduction through the copper of the heat sink and both conduction and forced convection in the air surrounding the heat sink. Natural convection was not incorporated into the simulation since it was assumed to have a negligible effect on the heat transfer of the heat sink compared to the effect of forced convection.

The initial temperature of the system was set at an ambient temperature of 20 °C , the default in COMSOL. A heat flux condition of 82W was set on a square centered on the bottom of the heat sink to represent the CPU, labeled above in Figure 4. The dimensions for the CPU

were not provided in the paper, but it was mentioned that the simulated CPU was a Pentium IV Processor for which the dimensions are provided online.[2]

Inflows and outflows were selected across the same boundaries as the inlet and outlet conditions for the Laminar Flow module. The inflow upstream conditions were left as the STP COMSOL defaults. Additionally, a thermal insulation layer was added across the base of the heat sink around where the CPU was located so that heat flowed out through the heat sink.

Mesh:

In order to iterate through a variety of simulations using different flow rate boundary conditions and fin arrangements quickly, we used the coarser mesh option in COMSOL. Given the narrow geometry of the heat fins (0.3 mm wide) relative to the overall geometry of the heat sink base (60mm by 83mm), the mesh can be seen below to be much finer on the fins. Only meshes for the straight model are shown as the meshes for the oblique models looked similar.

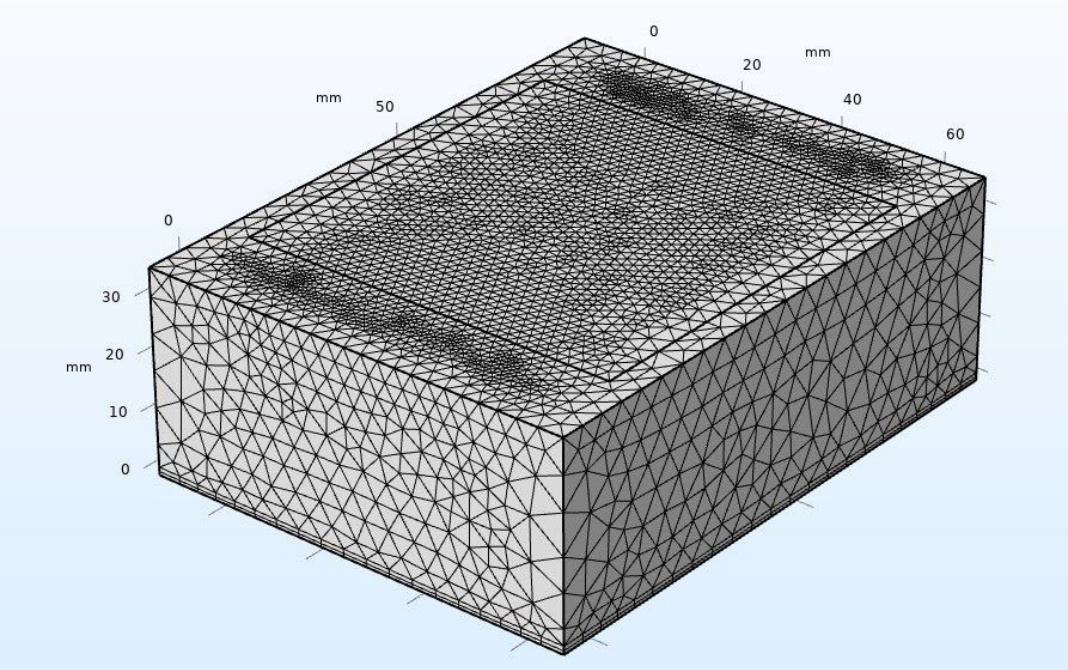

Figure 5. Mesh on Straight Fins Heat Sink Domain Geometry.
Mesh consists of 667,583 domain elements.

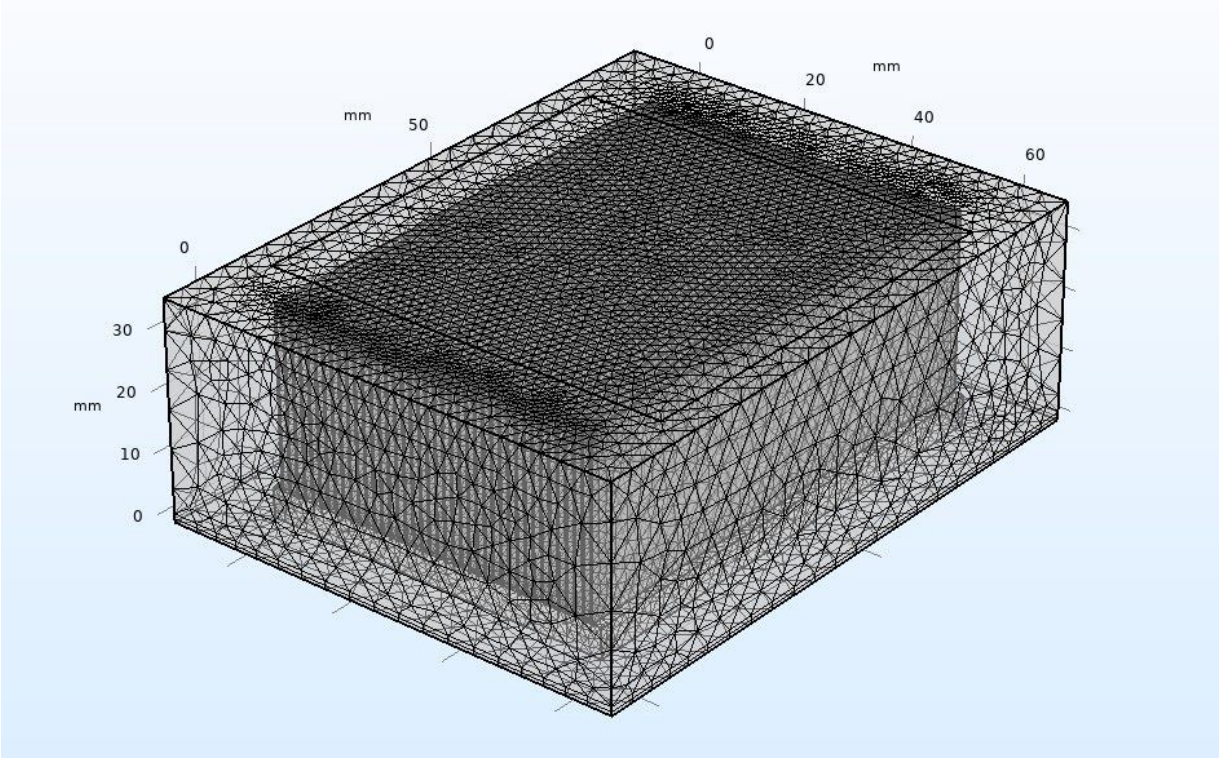

Figure 6. Translucent view of Mesh on Straight Fins Heat Sink Domain Geometry.

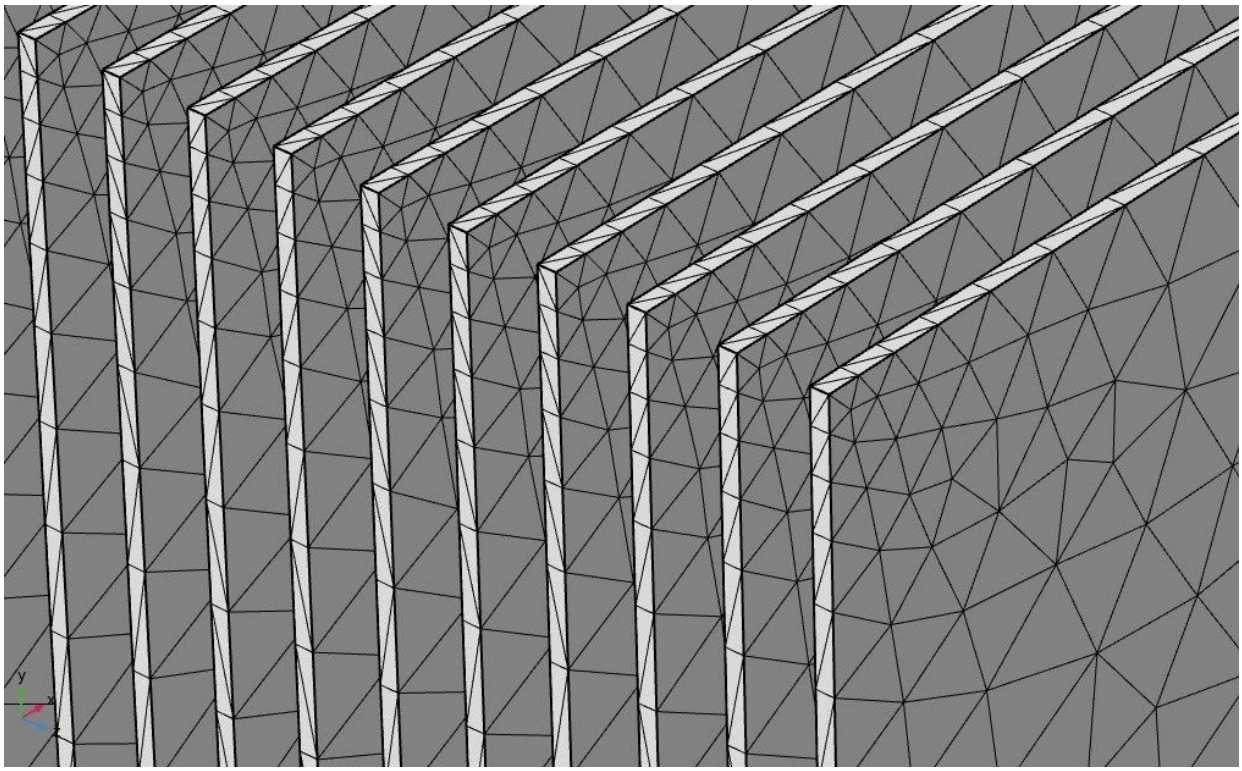

Figure 7. Magnified View of Mesh on Straight Fins Heat Sink Domain Geometry. Note the smaller mesh element size close to the fin tips.

Computation:

We ran a total of 15 simulations, consisting of three different flow rates through five different heat sink geometries. Each simulation took approximately 20 minutes to run, with simulations taking slightly longer at higher flow rates. Our convergence plots, such as the example provided below in Figure 8, showed that both flow and heat transfer parameters converged with little error.

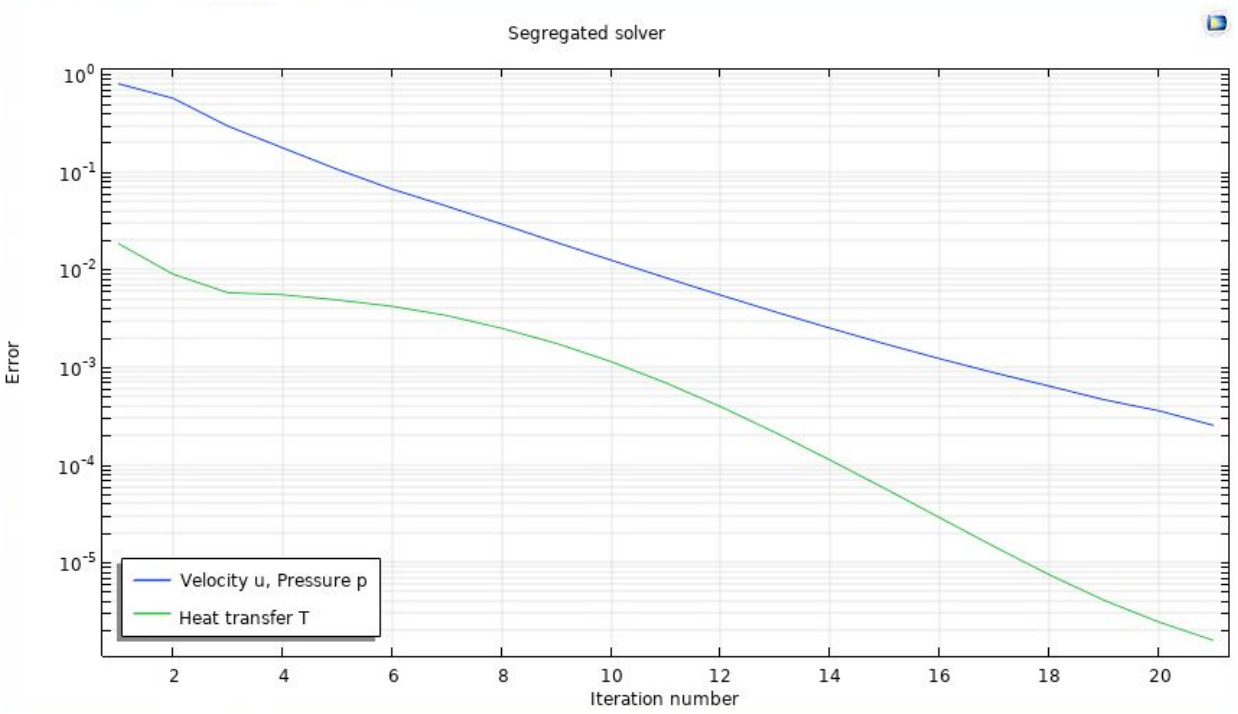

Figure 8. Example Convergence Plot from Simulation Using Straight Model at 10 CFM

3. Results and Validation

COMSOL Plots:

For each simulation, three plots were produced: one showing the flow and heat transfer through the system as a whole looking at a cross-section in plane with the fin surfaces, another showing the pressure distribution through a cross-section cutting through the fins, and another showing the temperature distribution through that same cross-section cutting through the fins. Since the focus of this analysis is how changing the heat fin angle affects the flow and heat transfer through the heat sink, plots are only included for simulations run at 10 CFM for brevity. Plots of the same type are presented together and have the same color scale for easy comparison between simulations.

Big Picture Plots:

The following plots illustrate the important flow and heat transfer concepts of the heat sinks analyzed. Cool ambient temperature air flows into the heat sink from the fan above while heat flows upwards and outwards from the CPU located at the bottom of the heat sink. Together the flow of cool air and heat contribute to the temperature distribution of air inside the heat sink. The average temperature distribution appears to be significantly greater for the straight model compared to the oblique models at the heat sink center where this temperature slice is taken. Although the straight model did appear to have a higher average temperature, this trend is likely overexaggerated in the plots below due to the gap formed between fins in the heat sink center in oblique models, not present in the straight model.

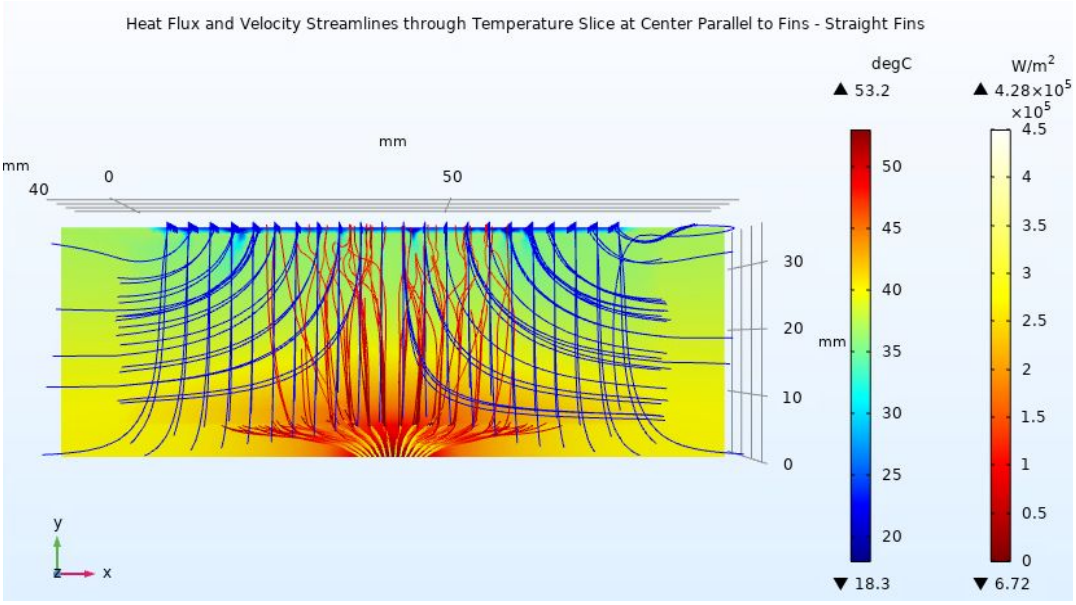

Figure 9. Big Picture Plot - Straight Model at 10 CFM

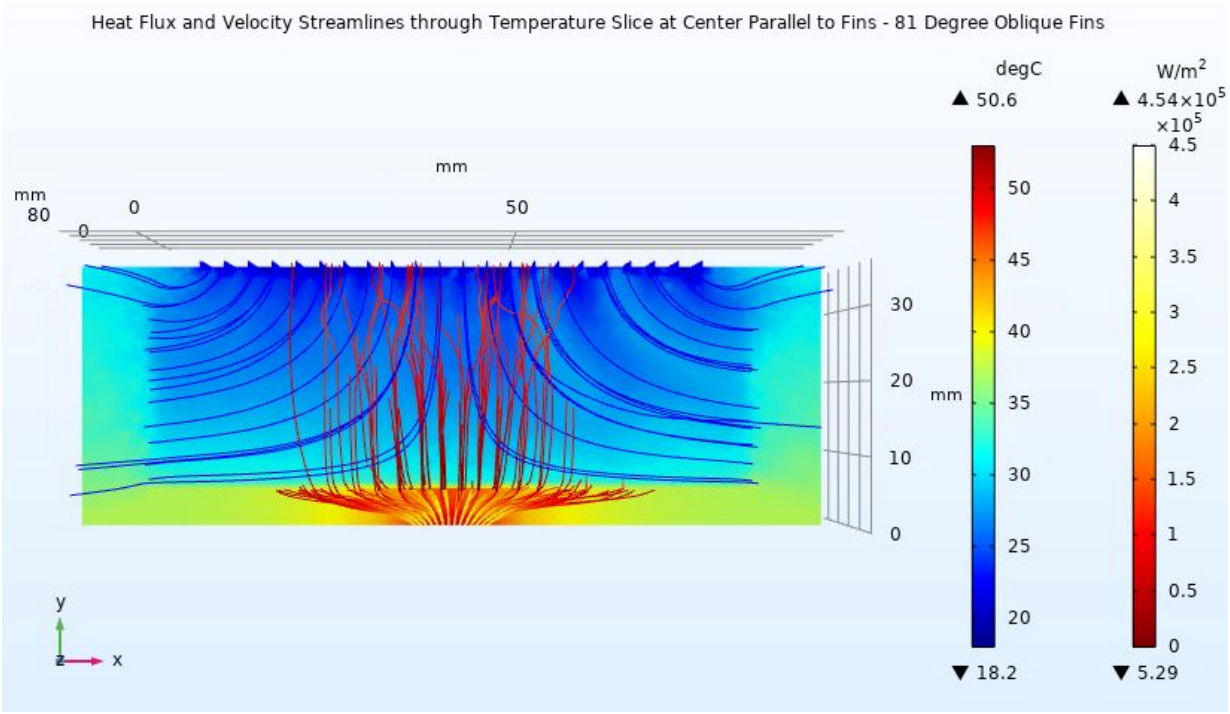

Figure 10. Big Picture Plot - Oblique Model (α = 81°) at 10 CFM

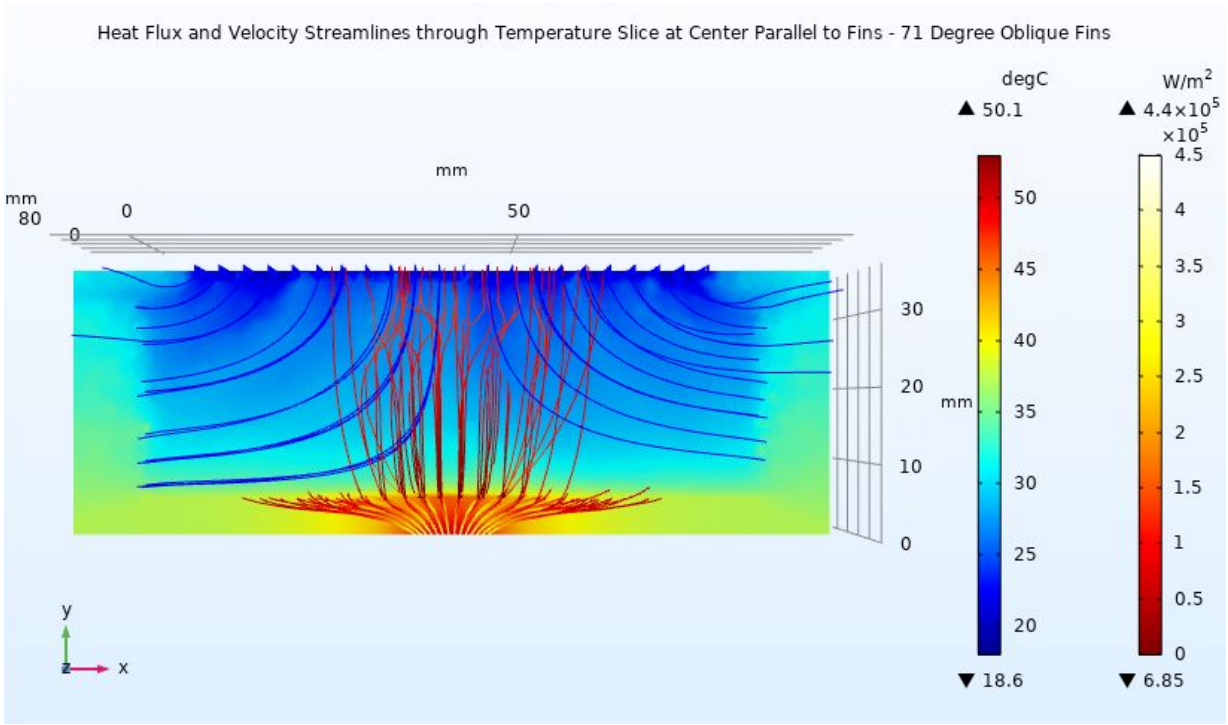

Figure 11. Big Picture Plot - Oblique Model (α = 71°) at 10 CFM

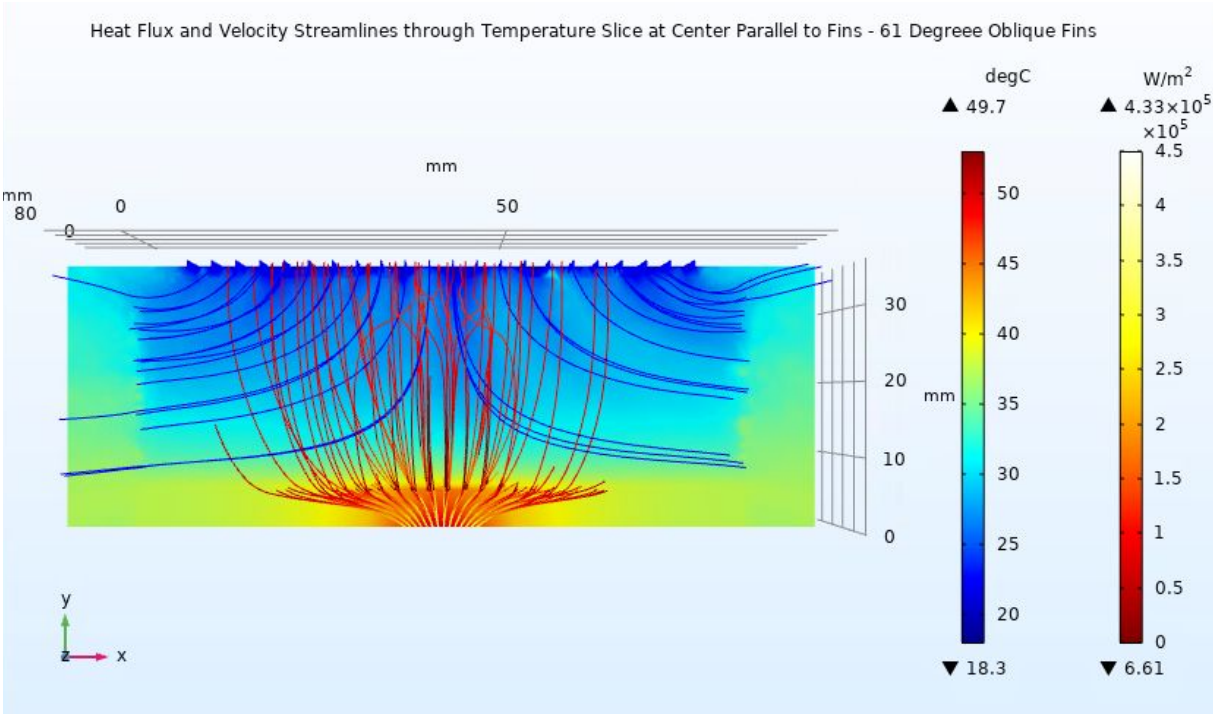

Figure 12. Big Picture Plot - Oblique Model (α = 61°) at 10 CFM

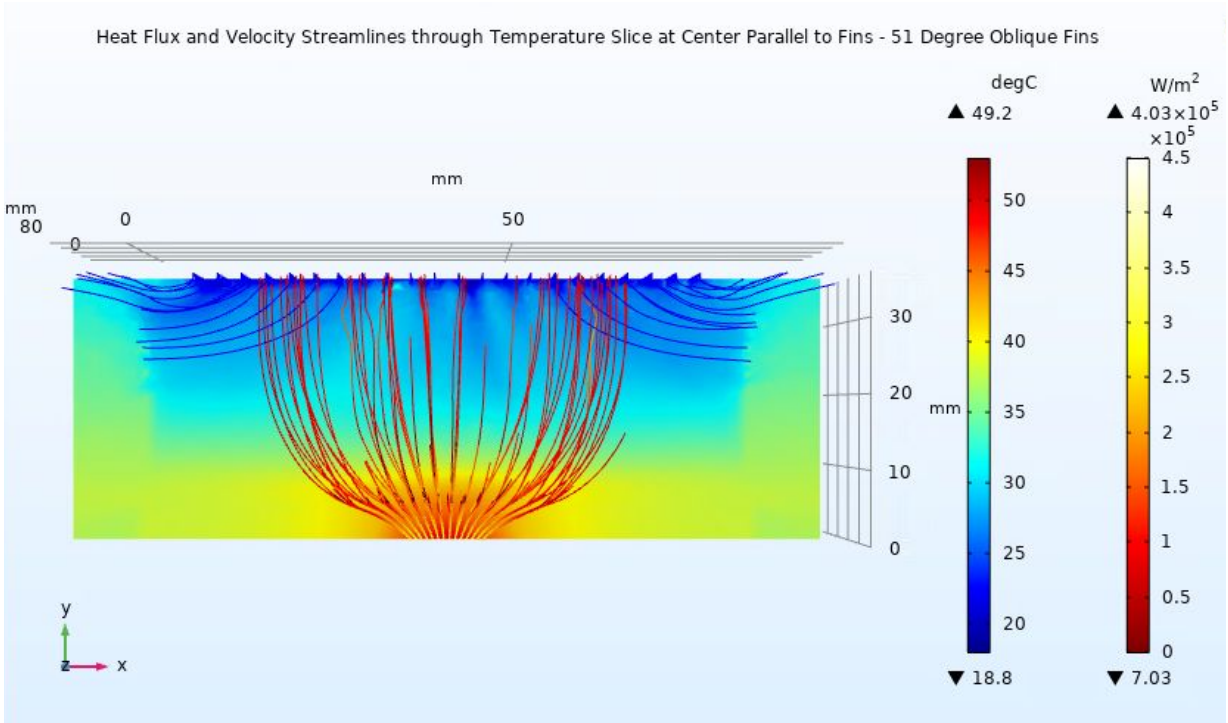

Figure 13. Big Picture Plot - Oblique Model (α = 51°) at 10 CFM

Cross-Sectional Pressure Plots:

The following plots illustrate the pressure distribution for a cross-sectional slice cutting through the fins at the heat sink center. As was discussed in the paper used for model validation, pressure is one of the most important flow parameters determining the efficiency of the heat sink.

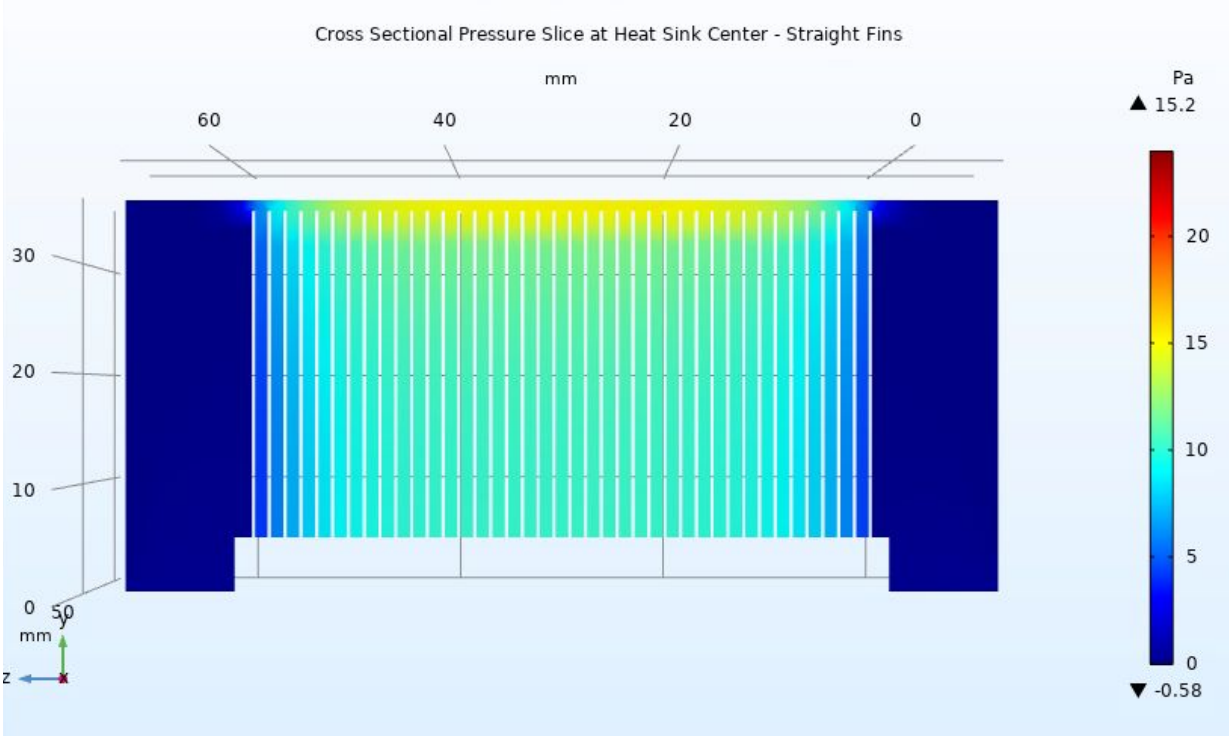

Figure 14. Plot of Pressure at Fin Cross-Section - Straight Model at 10 CFM

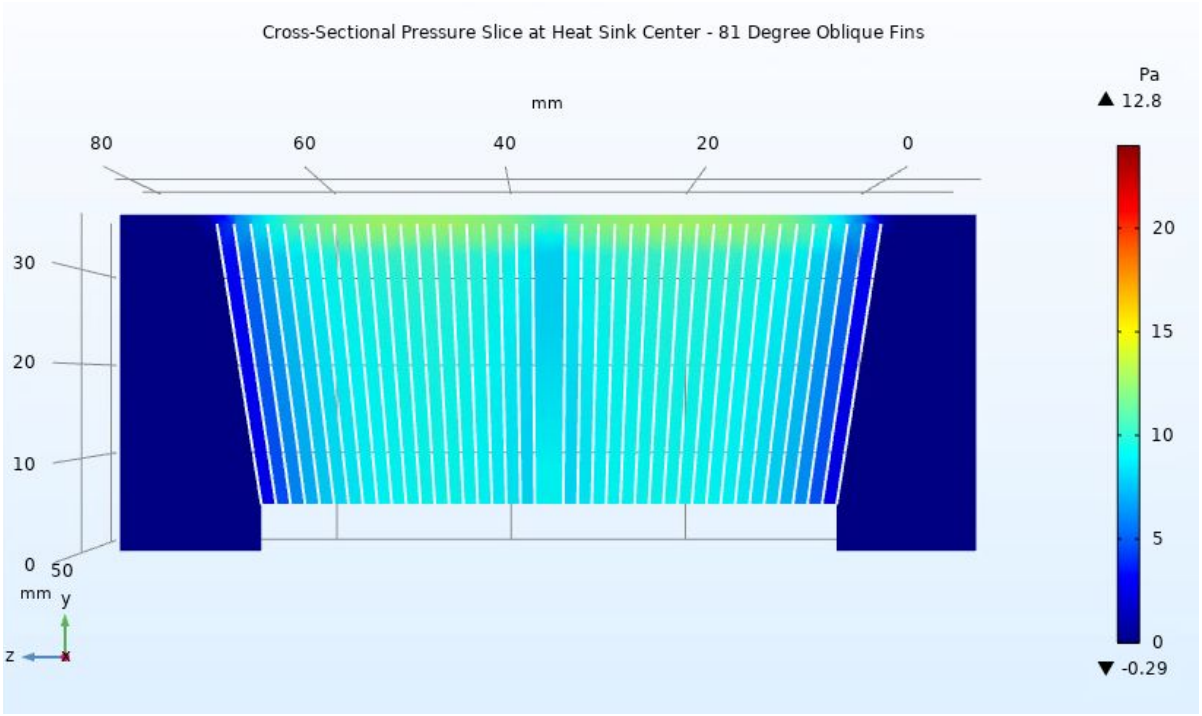

Figure 15. Plot of Pressure at Fin Cross-Section - Oblique Model (α = 81°) at 10 CFM

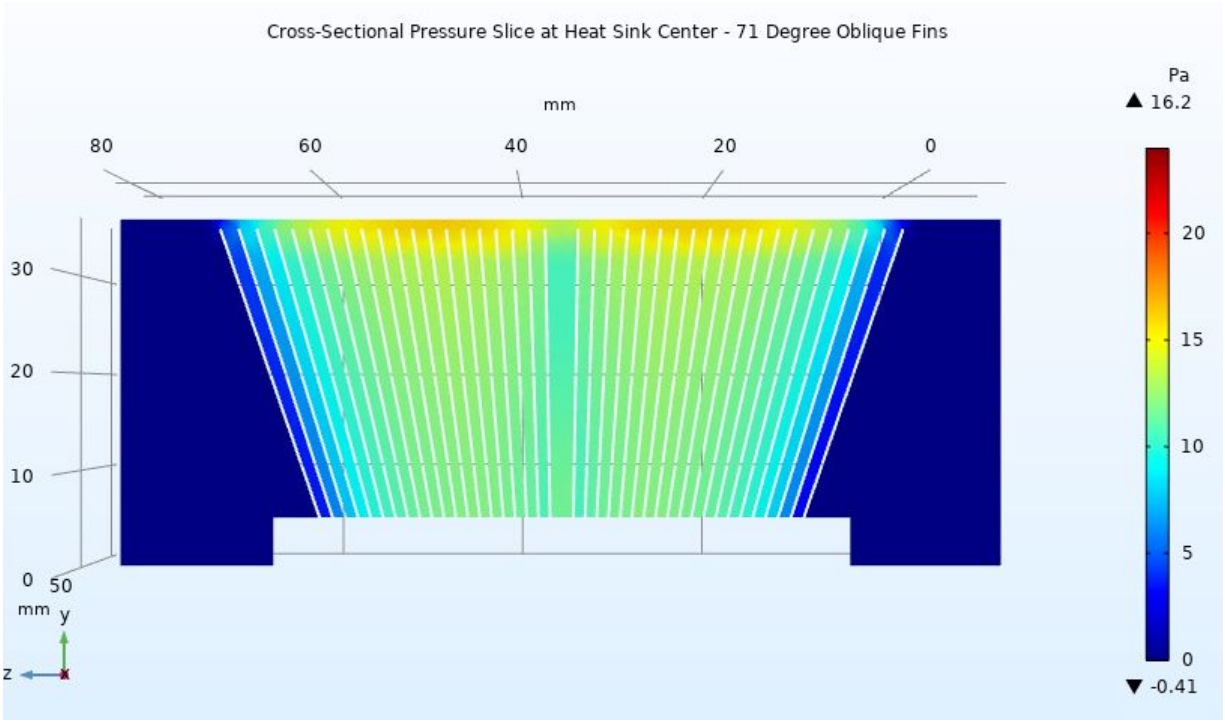

Figure 16. Plot of Pressure at Fin Cross-Section - Oblique Model (α = 71°) at 10 CFM

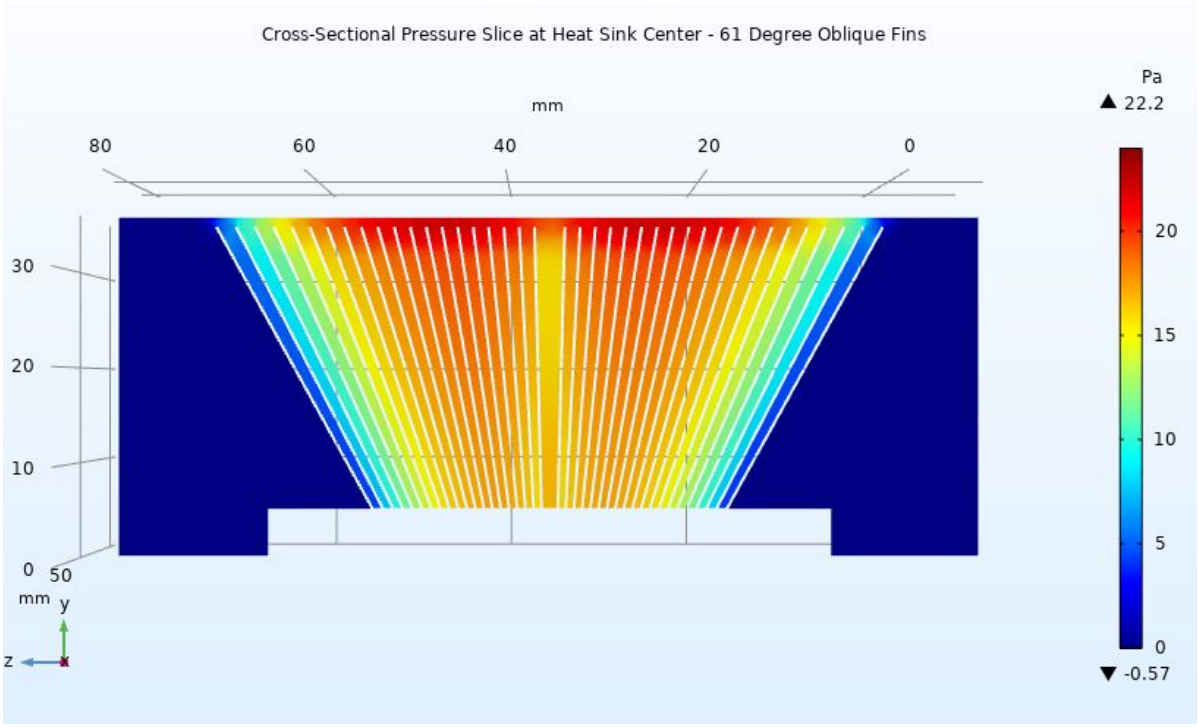

Figure 17. Plot of Pressure at Fin Cross-Section - Oblique Model (α = 61°) at 10 CFM

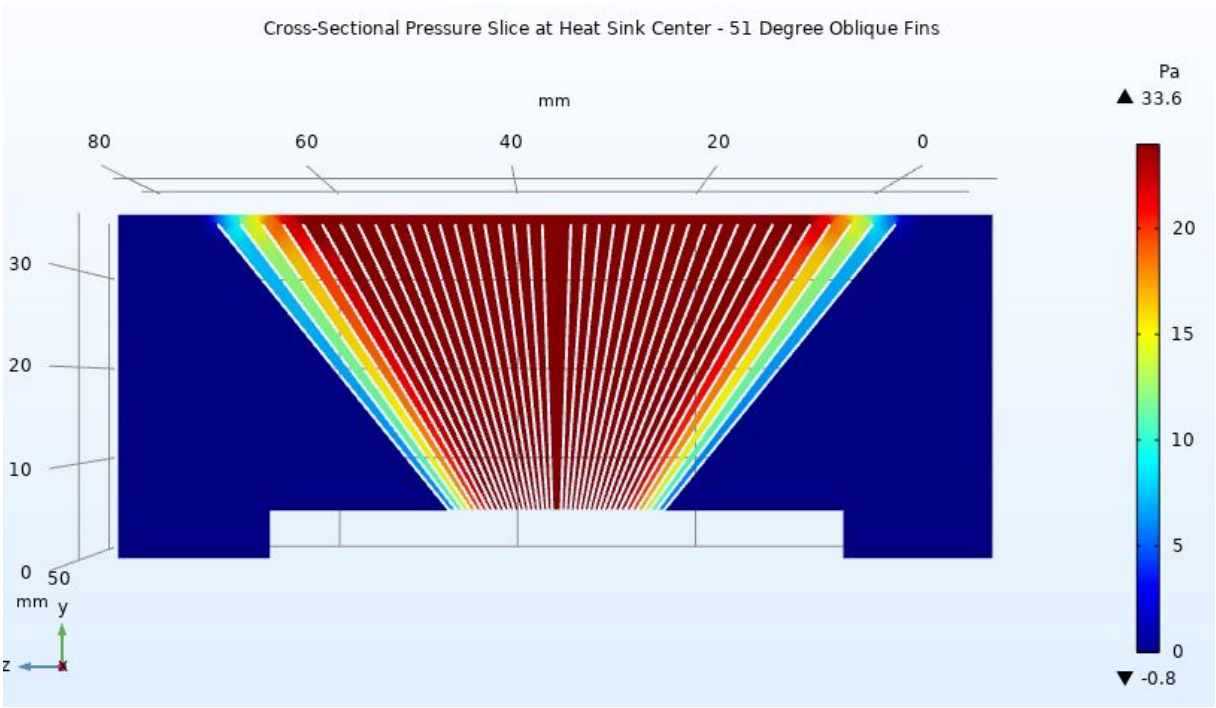

Figure 18. Plot of Pressure at Fin Cross-Section - Oblique Model (α = 51°) at 10 CFM

Cross-Sectional Temperature Plots:

The following plots illustrate the temperature distribution for a cross-sectional slice cutting through the fins at the heat sink center. Examining areas where the color changes rapidly and thus there is a high temperature gradient, locations of more efficient heat transfer can be identified. Additionally, these plots are a useful indicator for whether the CPU or other nearby electronic components will overheat and fail.

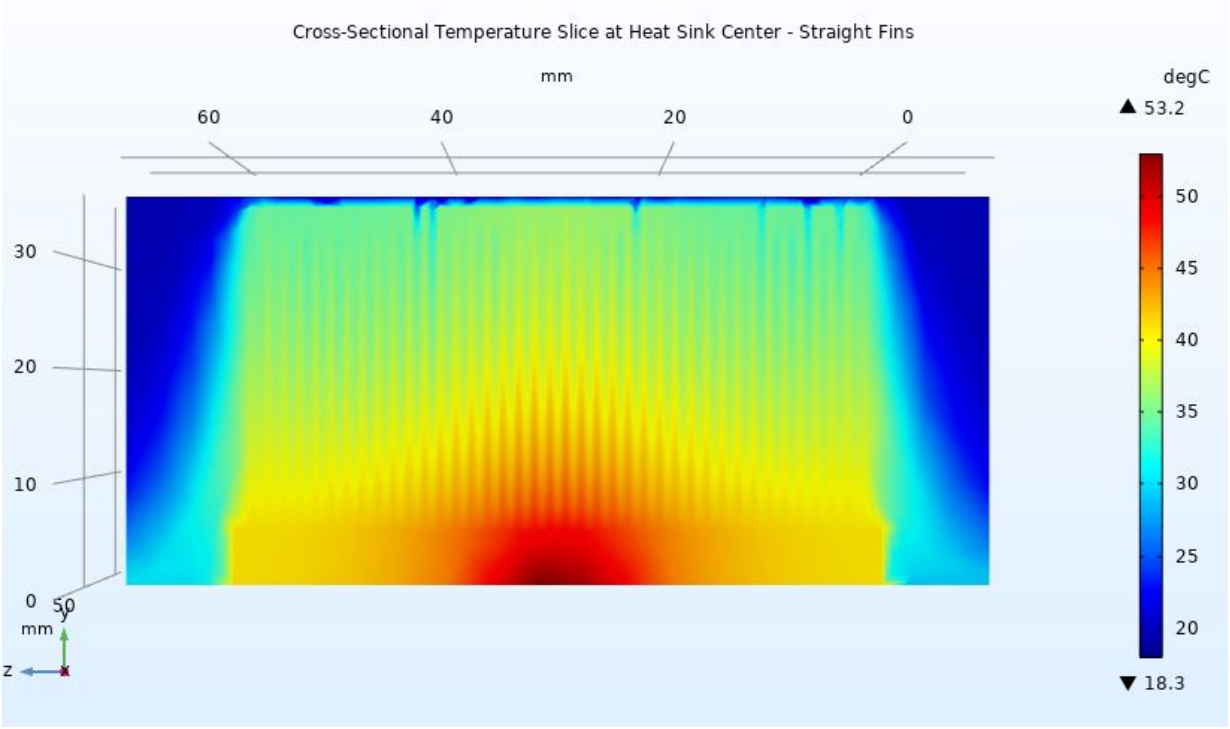

Figure 19. Plot of Temperature at Fin Cross-Section - Straight Model at 10 CFM

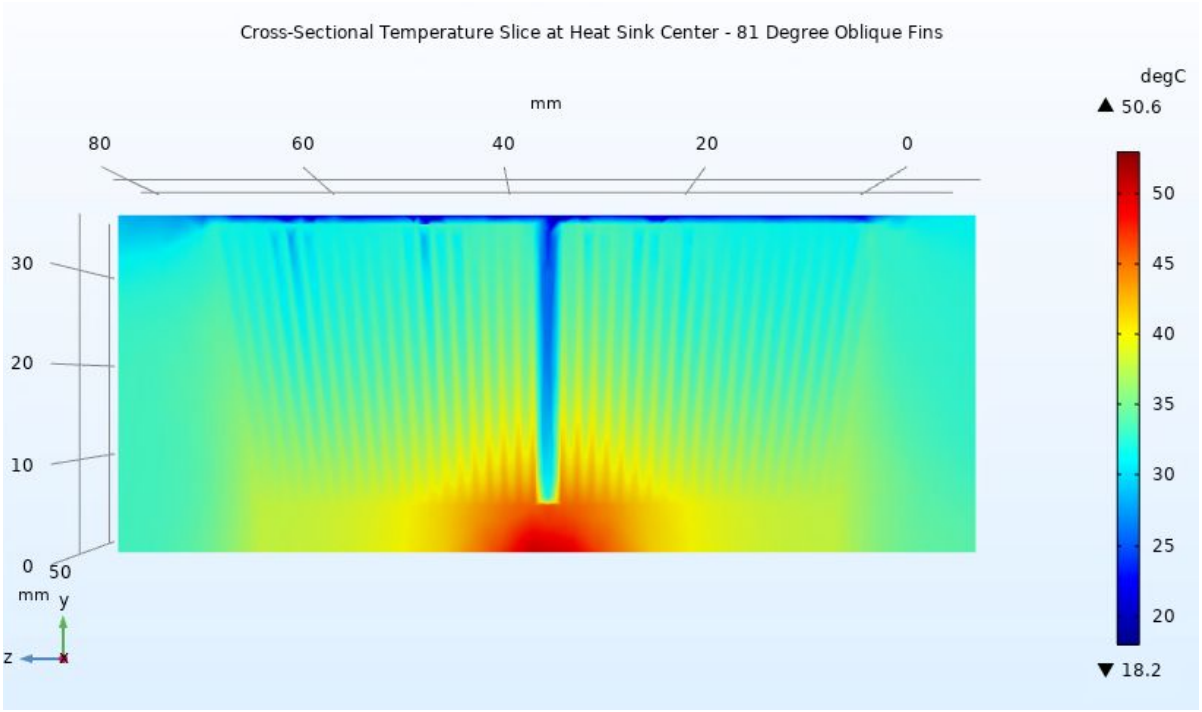

Figure 20. Plot of Temperature at Fin Cross-Section - Oblique Model (α = 81°) at 10 CFM

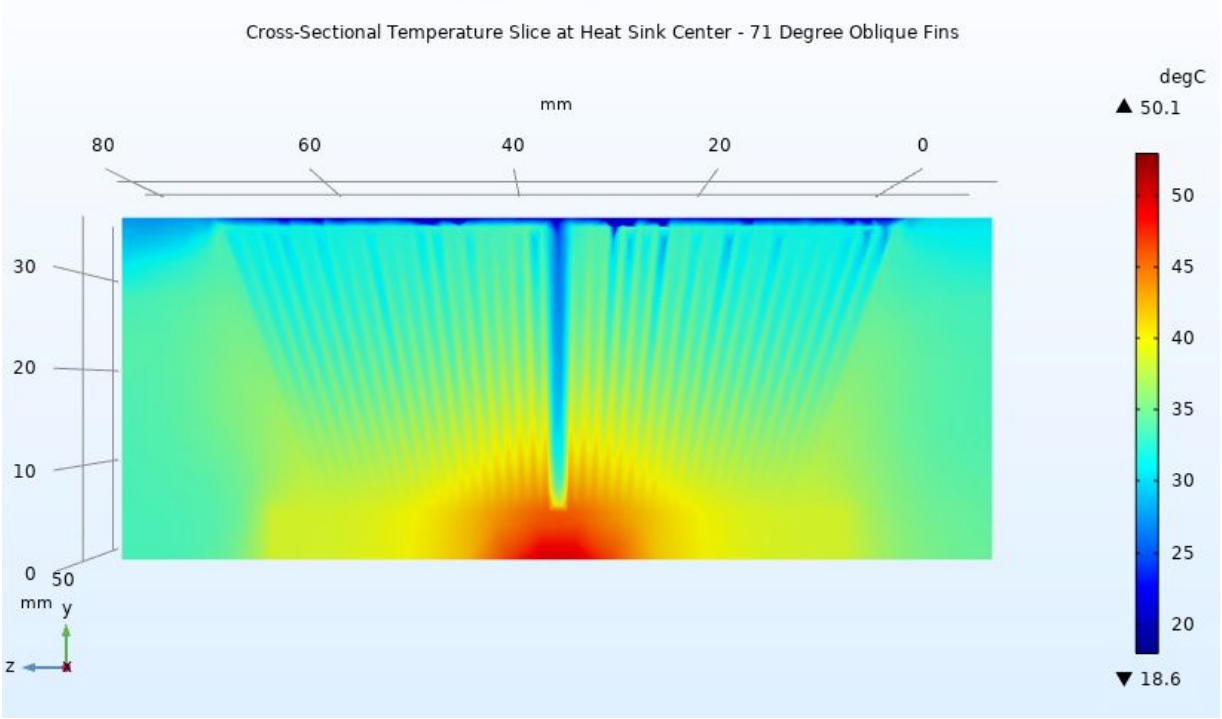

Figure 21. Plot of Temperature at Fin Cross-Section - Oblique Model (α = 71°) at 10 CFM

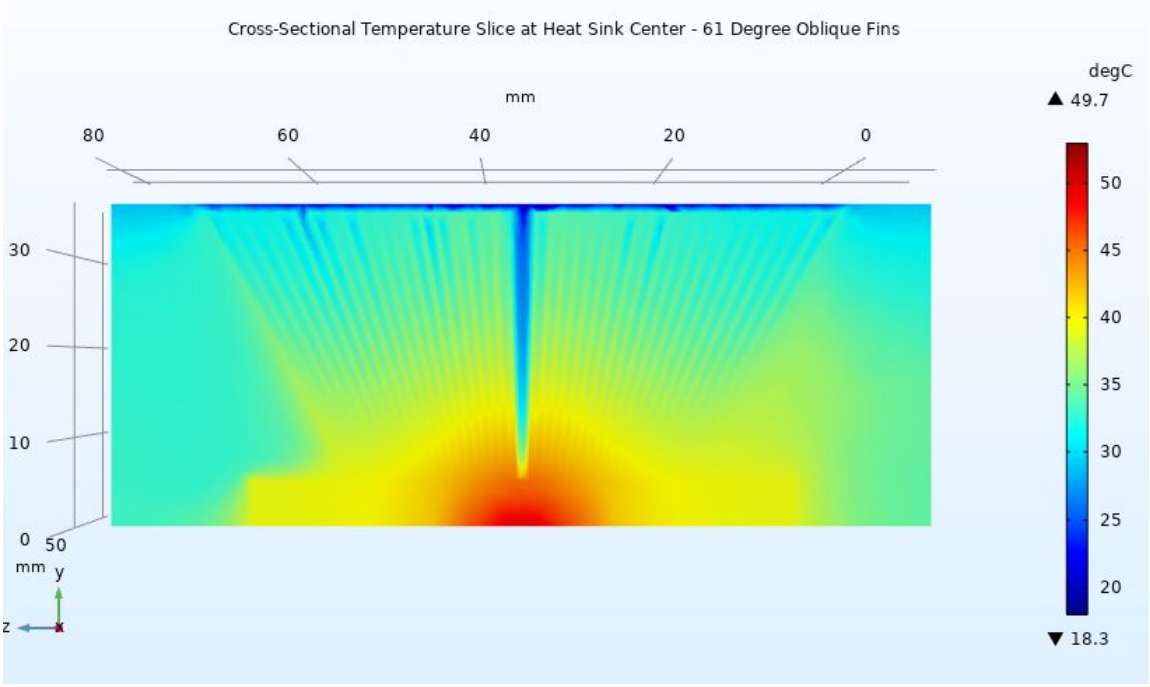

Figure 22. Plot of Temperature at Fin Cross-Section - Oblique Model (α = 61°) at 10 CFM

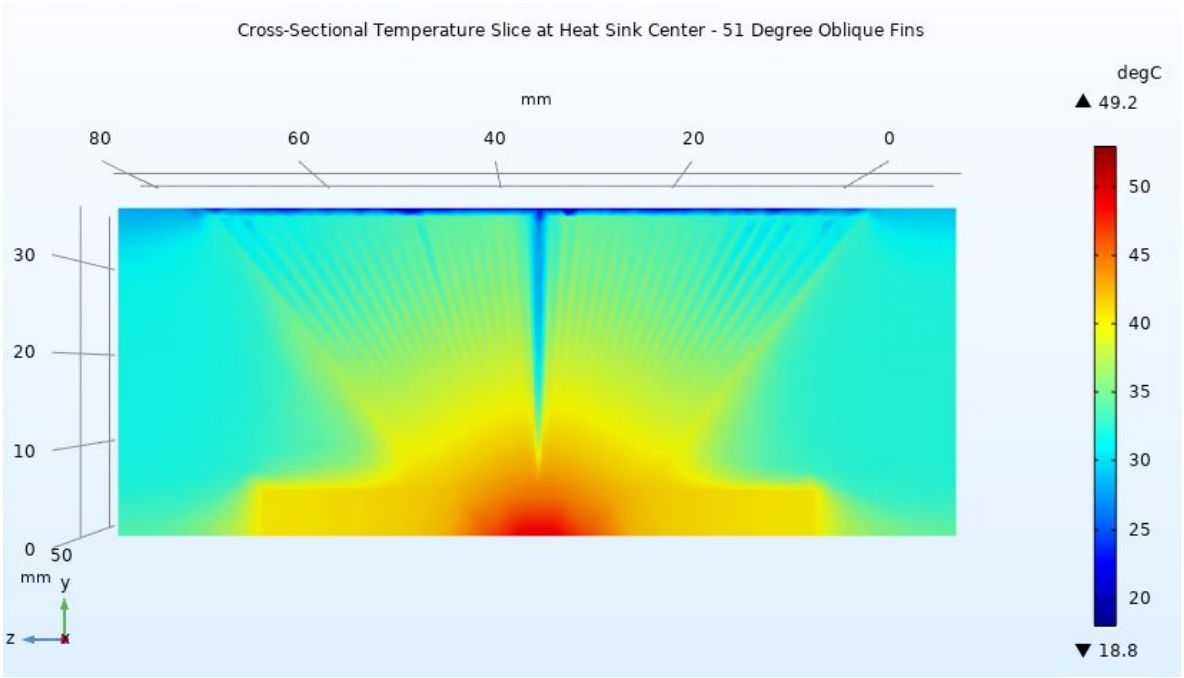

Figure 23. Plot of Temperature at Fin Cross-Section - Oblique Model (α = 51°) at 10 CFM

Numerical Results:

For each simulation, the maximum pressure in the air domain (equivalent to the pressure drop across the heat sink since pressure outside the heat sink was zero gauge pressure) and average temperature on the CPU surface were recorded. Using the CPU temperature, the thermal resistance of the heat sink was then calculated using the following expression from the paper used for model validation: $R_{th} = \frac{T_{CPU} - T_{ambient}}{Q_{dot,\,CPU}}$, where $T_{ambient}$ is 20 ℃ and $Q_{dot,\,CPU}$ is 82W. These values are tabulated below in Table 1 for all simulations.

Geometry	Flow Rate (CFM)	Max Pressure (Pa)	CPU Temperature (℃)	Thermal Resistance (℃/W)
Straight Fins, α=90°	10	15.206	50.441	0.371
	20	43.630	41.403	0.261
	30	84.851	38.426	0.225
Oblique Fins, α=81°	10	12.846	47.816	0.339
	20	39.147	40.351	0.248
	30	78.206	37.887	0.218
Oblique Fins, α=71°	10	16.225	47.7	0.338
	20	48.334	40.145	0.246
	30	95.336	37.639	0.215
Oblique Fins, α=61°	10	22.232	47.346	0.333
	20	65.220	39.763	0.241
	30	127.20	37.224	0.210
Oblique Fins, α=51°	10	33.646	47.176	0.331
	20	98.411	39.566	0.239
	30	190.45	37.009	0.207

Table 1. Relevant Heat Sink Efficiency Simulation Data

Using the data tabulated above in Table 1; pressure, CPU temperature, and thermal resistance are plotted as functions of flow rate and fin angle on the following plots.

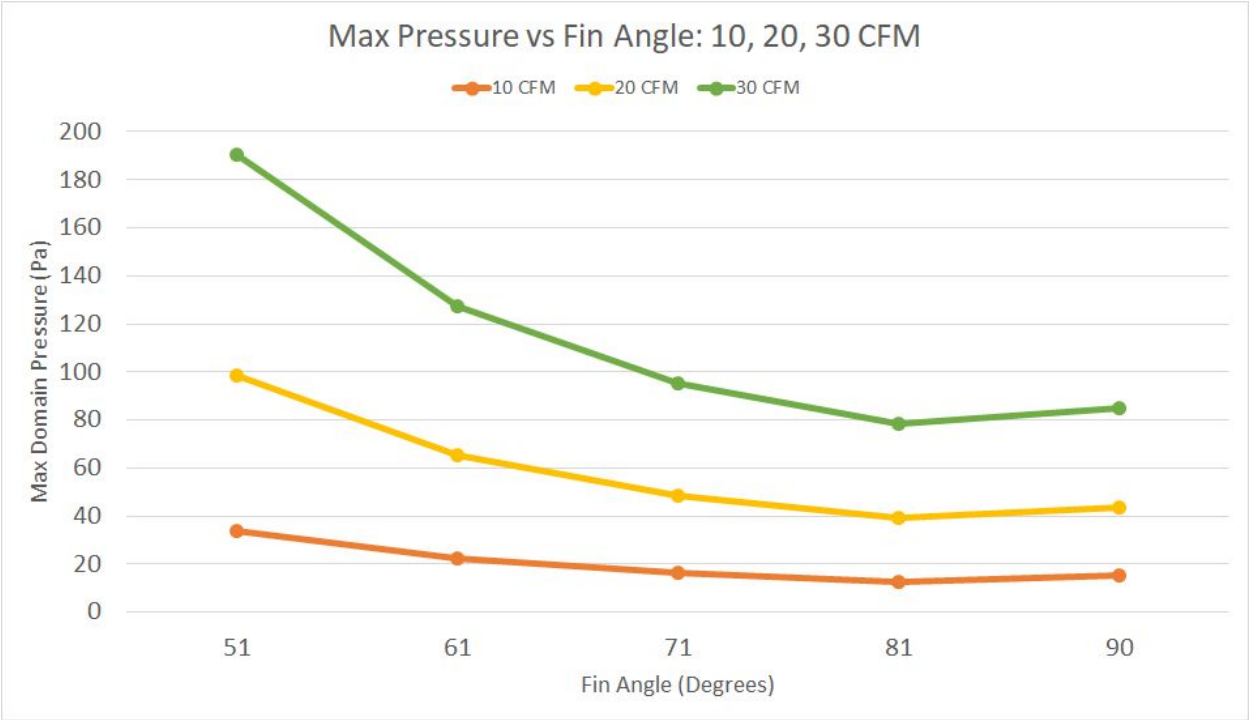

Figure 24. Max Domain Pressure at Different Fin Angles and Flow Rates. Note that pressure increases as fin angle decreases (becomes more oblique), except from 81 to 90 degrees. Given that the 81 degree oblique model has the lowest pressure, it is expected to be the most efficient.

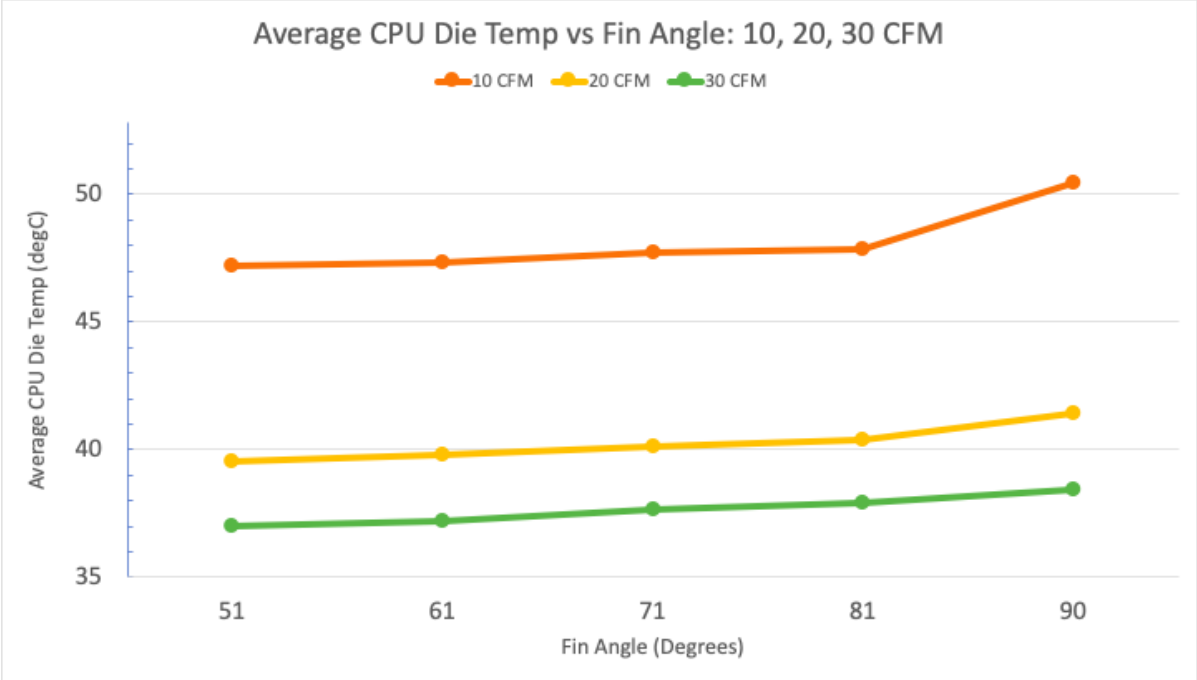

Figure 25. CPU Temperature at Different Fin Angles and Flow Rates. Note the steep decrease from 90 to 81 degrees followed by minimal decreases for smaller oblique angles, enhanced at lower flow rates.

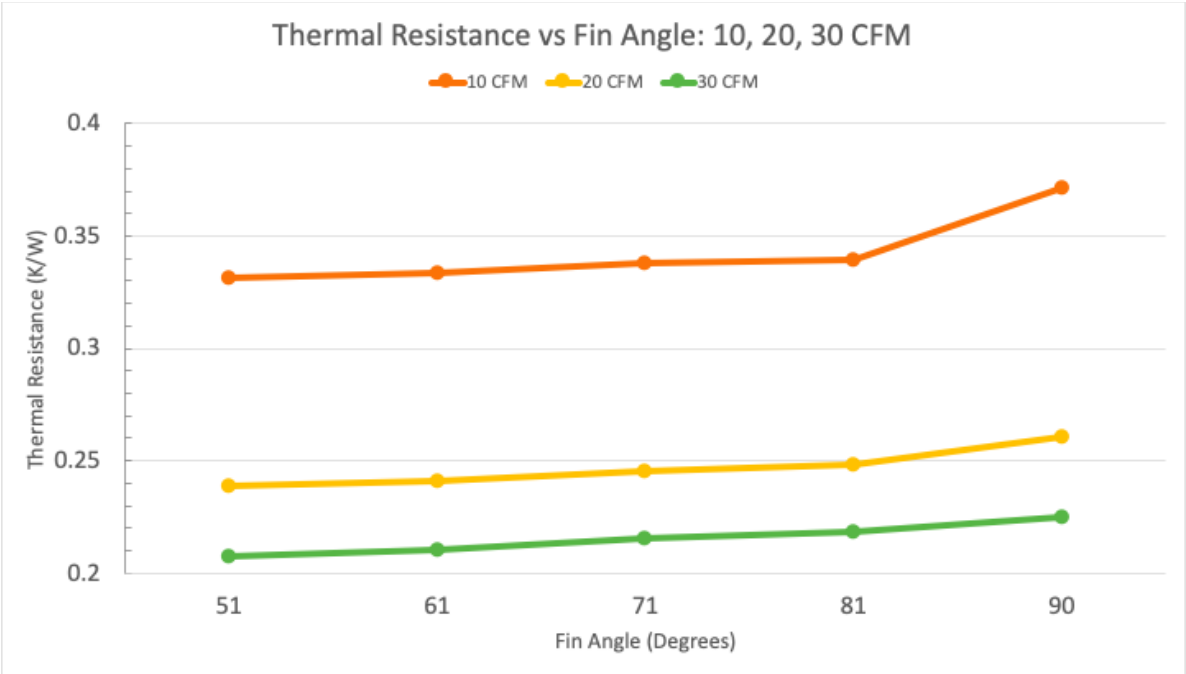

Figure 26. Thermal Resistance at Different Fin Angles and Flow Rates. Note similar curve shapes to Figure 25 since thermal resistance is proportional to CPU temperature.

Discussion:

Examining the temperature and thermal resistance data, it is evident that heat sinks with oblique fins are better suited for cooling CPUs than heat sinks with straight fins. Looking at Figures 25 and 26, it can be seen that the straight model had significantly higher CPU temperatures and thermal resistances across all three flow rates. The thermal resistance of the straight model was 11%, 7%, and 6% higher than the average oblique model thermal resistance for flow rates at 10 CFM, 20 CFM, and 30 CFM respectively. This result indicates that the straight model would be more likely to lead to CPU overheating given its higher resistance to heat transfer, particularly when using a less powerful fan. Although the paper used for model validation indicated that lower heat sink pressures would allow for more efficient heat sinks, no apparent correlation was found between pressure and heat transfer data.

An interesting result from the data was that there was not a significant improvement in the efficiency of the oblique heat sinks as the fin angle increased. This can be seen in Figures 25 and 26, where the slope of the lines are relatively shallow from 51 to 81 degrees compared to the steep increase in temperature and thermal resistance from 81 to 90 degrees. From 81 to 51 degrees, there was only a 2%, 4%, 5% decrease in thermal resistance for flow rates of 10 CFM, 20 CFM, and 30 CFM respectively. It is also worthwhile to note that this trend in thermal resistance decreasing with flow rate is the opposite of the relationship between flowrate and thermal resistance mentioned earlier between 81 and 90 degrees. In other words, the benefit of using an oblique model over a straight model decreases with flow rate while the benefit of using a more extreme oblique model over another oblique model increases with flow rate. All in all, it appears that there is little heat transfer benefit in using a heat sink with more extreme oblique angles. Furthermore, more extreme oblique angles would already be undesirable as they are likely more difficult to manufacture.

There is also a strong correlation between heat transfer performance of the heat sinks and flow rate. This is an expected result as higher flow rates maintain a higher temperature gradient in the heat sink by bringing in cool air faster, allowing the heat sink to transfer heat more effectively.

Validation

The journal paper selected to validate the model was titled *Experimental study of the heat sink assembly with oblique straight fins*. As the title suggests, the authors constructed an experiment to record data for a heat sink assembly with straight fins and a heat sink assembly with oblique fins. An axial fan (blowing air down onto the heat sink base as opposed to across the heat sink base) was mounted on top of each heat sink and a heat source simulating a CPU was added underneath the heat sink. Data was recorded for the straight fin and oblique fin heat sinks using two different fans at a variety of fan speeds. For the purposes of model validation, the focus of the paper is unfortunately just the heat transfer and not so much the flow through the

heat sink. The main experimental data that was obtained included data on heat sink base temperature, heat sink thermal resistance, and noise. This data is included below in Figure 27.

Thermal performances and noises of the heat sink assemblies

Fin Type	Fan	rpm	T_C (°C)	Ψ_{CA} (°C/W)	Noise (dBA)		
					P1	P2	P3
Oblique	NTUST	2000	81.4	0.48	26.4	20.6	21.0
		2500	73.2	0.38	29.7	27.2	27.1
		3000	70.7	0.35	34.2	29.5	29.7
		3500	69.9	0.34	39.2	35.0	34.4
		4000	69.1	0.33	42.2	38.1	38.2
	Reference	2000	83.0	0.50	27.1	20.4	20.5
		2500	75.6	0.41	31.2	27.0	26.9
		3000	71.5	0.36	36.0	29.9	29.7
		3500	70.7	0.35	39.4	33.7	33.1
		4000	69.9	0.34	43.0	36.9	36.4
Vertical	NTUST	2000	87.1	0.55	26.1	22.1	22.5
		2500	75.6	0.41	30.9	27.0	27.1
		3000	73.2	0.38	36.5	30.0	29.5
		3500	71.5	0.36	40.4	34.5	34.1
		4000	69.9	0.34	43.0	38.2	37.5
	Reference	2000	90.4	0.59	28.5	21.7	21.4
		2500	78.9	0.45	33.4	26.7	26.9
		3000	74.0	0.39	38.0	29.7	29.5
		3500	72.3	0.37	42.0	32.1	33.0
		4000	70.7	0.35	45.3	36.6	35.6

Figure 27. Experimental Heat Transfer and Noise Data from Research Paper

Looking at the thermal resistances recorded above in Figure 27, the thermal resistances at different fan speeds using two different fans ranged from 0.33 to 0.50 ℃/W for the oblique model (α = 71°) and 0.34 to 0.59 ℃/W for the straight model. In the model, thermal resistances at different flow rates ranged from 0.215 to 0.339 ℃/W for the oblique model (α = 71°) and from 0.225 to 0.371 ℃/W for the straight model. Not only are these ranges of thermal resistance similar in magnitude and overlapping, but they also reflect the higher range of thermal resistances for the straight model compared to the oblique model seen in the paper. Although the CPU temperatures and thermal resistances of the model are of smaller magnitude than the experimental data from the paper, the trends in data between fin arrangements still appear to be well represented. Therefore, the model is well validated as a tool in determining the relationship between heat transfer and fin angle even though the temperatures and thermal resistances reported may be inaccurate.

On the other hand, the lack of flow data made it difficult to validate how the flow was modeled through the heat sinks. However, experimental data was provided in the paper on the pressure output by the fans at different speeds and thus flow rates. This data is included below in Figure 29.

The performance of fans at different rotating speeds

Rotating speeds (rpm)	2000	3000	4000
Reference fan			
Performance			
Ps (mm Aq)	1.14	2.57	4.56
Q (CFM)	18.5	27.8	37.1
Noise (dBA)			
Position 1	22.8	30.8	37.0
Position 2	23.5	31.6	37.8
Position 3	22.1	30.3	36.5
NTUST fan			
Performance			
Ps (mm Aq)	1.47	3.30	5.86
Q(CFM)	15.7	23.5	31.4
Noise (dBA)			
Position 1	21.7	29.9	36.1
Position 2	22.5	30.6	36.8
Position 3	21.4	29.5	35.7

Figure 28. Fan Performance Data from Research Paper.

Examining the differences between the experimental pressure output of the fan and the simulated pressure entering the heat sink assembly, the maximum pressure in the domain, the flow data of the model can be verified indirectly. Looking at the pressures recorded above in Figure 30, the pressures for the two different fans ranged from 1.14 to 5.86 mm Aq for flow rates from 15.7 CFM to 37.1 CFM. In the model, pressures ranged from 1.31 to 19.4 mm Aq for flow rates from 10 CFM to 30 CFM. Although the range of pressures recorded in the model is dramatically larger than the pressures recorded in the paper, the results are still of similar magnitude, allowing for validation of the flow data of the model. Even so, it would have been better to find another research paper with experimental data regarding flow through a heat sink with which to validate our model through more direct and legitimate means.

Reviewing the validation of the model's heat transfer and flow data, there are a number of reasons why the experimental data may not exactly match the simulation data. In terms of the heat transfer data, one explanation for the experimental CPU temperature and thermal resistance data being higher than the results recorded in the model is that the material heat transfer properties (conductivity and convective heat transfer coefficient) of the copper heat sink and surrounding air were overestimated in the model.

In terms of the flow data, one explanation for the experimental pressure data being lower than the model pressure data is that the pressure data provided for the fan in the experiment is actually recorded as a static pressure rather than as a total pressure. This would lead to lower experimental pressures since static pressure would be lower than the total pressure since the total pressure is the sum of the static and dynamic pressures. However, it is unlikely this difference alone accounts for the significantly different pressure data.

Given these potential explanations for the validation error and the similar magnitude flow and heat transfer results between the model and experiment, it is likely that the model as a whole is representative of the experimental heat sink system. Whether the experimental setup is itself realistic is a separate question. Regrettably, this is a serious concern for this paper as several conflicting ideas were presented in the paper. Specifically the dimensioned drawings of the heat sink geometry differed with what was written about the heat sink geometry in the text of the paper and the pressure vs. flow rate data recorded in Figure 10 and Table 2 of the paper presented opposing trends.

4. Conclusions and Future Work

The purpose of this analysis was to determine the effect of oblique fins, as an alternative to straight fins, on the thermal performance of a heat sink. The simulation results show that oblique fins experience higher pressures when subjected to the same flow conditions, but improve heat transfer overall and reduce CPU die temperature. These results confirmed the paper's findings that oblique finned assemblies perform better in heat transfer, but refuted the paper's finding that oblique fins experience lower pressures. It was also found that the benefit in heat transfer when using oblique fins instead of straight fins is reduced at higher flow rates and further reductions in fin angle from an oblique model provided minimal improvements in heat transfer.

Many challenges were encountered when trying to produce an appropriate model of the heat sink. The paper selected for model validation disagreed on dimensions for the heat sinks making it unclear whether the modeled heat sinks were faithful to the experimental setup. Additionally, the paper presented the data using a slightly different format making it more difficult to compare results. For example, the paper reported heat transfer parameters as a function of fan speed instead of as a function of flow rate and pressure were reported as static pressures instead of total pressures. Despite these challenges, the simulation and experimental results were of comparable magnitude, covering a similar range of values under similar boundary conditions. For this reason the model was accepted as being validated by the experimental results presented in the research paper. Had more time been available, it would have been worthwhile to investigate another research study with experimental data on flow through a heat sink as the validation used for the flow data in this model was produced using an indirect and questionable method.

The key takeaway from this study is that, in low flow rate conditions (less than 30 CFM), there are large gains to be made in efficiency with a small change to geometry. This conclusion could be useful for heat sink manufacturers and the electronics industry as a whole. Our data shows that a heat sink can be 3 to 9 percent more efficient, with greater benefits occurring at slower flower rates, just by adding a 9 degree pitch to the fins. This is good news for manufacturers as adding a 9 degree pitch may be as simple as designing a new wedge-shaped die through which the heat sink could be extruded. Based on the model data, one explanation for why the benefit of using an oblique fin heat sink decreases at higher flower rates is that pressure also increases at higher flow rates, perhaps cancelling the benefits of the oblique geometry.

These promising results prompt questions for future work. If a small angle change led to significant heat transfer benefits, what would heat transfer data from the range of angles between 90 degrees and 81 degrees look like? Is there an optimal balance between manufacturability and

efficiency increase somewhere in that range? What about testing other geometries, like parabolic or spherical-shaped fins?

5. Citations:

1. Lin, Sheam-Chyun, et al. “Experimental Study of the Heat Sink Assembly with Oblique Straight Fins.” *Experimental Thermal and Fluid Science*, vol. 29, no. 5, Jan. 2004, pp. 591–600.

2. “Intel® Pentium® 4 Processor Supporting HT Technology 3.40E GHz, 1M Cache, 800 MHz FSB Product Specifications.” *Intel Product Specifications*, ark.intel.com/content/www/us/en/ark/products/27505/intel-pentium-4-processor-supporting-ht-technology-3-40e-ghz-1m-cache-800-mhz-fsb.html.